Inorganica Chimica Acta 363 (2010) 1425–1434

Contents lists available at ScienceDirect

Inorganica Chimica Acta

journal homepage: www.elsevier.com/locate/ica

Preparation, characterization and reactivity of 1-benzylpyridinium-4-aldoxime chloride and 1-phenacylpyridinium-4-aldoxime chloride and their complexes with the aquapentacyanoferrate(II) ion

Blaženka Foretić [a,*], Igor Picek [a], Ivica Đilović [b], Nicoletta Burger [a]

[a] Department of Chemistry and Biochemistry, Faculty of Medicine, University of Zagreb, Šalata 3, 10000 Zagreb, Croatia
[b] Department of Chemistry, Faculty of Science, University of Zagreb, Horvatovac 102a, 10000 Zagreb, Croatia

ARTICLE INFO

Article history:
Received 7 July 2009
Received in revised form 22 January 2010
Accepted 26 January 2010
Available online 4 February 2010

Keywords:
Substituted pentacyanoferrates(II)
Oximes
Pyridinium-4-aldoximes
Carbonyl compounds
Spectroscopy
Ionization constants

ABSTRACT

A detailed structural characterization of the biologically active 1-benzylpyridinium-4-aldoxime chloride and 1-phenacylpyridinium-4-aldoxime chloride was performed using NMR and vibrational and electronic spectroscopy, as well as X-ray diffraction. The complexes of these compounds with the aquapentacyanoferrate(II) ion were examined in solution, isolated as solids and characterized by elemental analysis, electronic, FT-IR and NMR spectral data. They were found to be mononuclear substituted pentacyanoferrates(II) containing the aldoxime group coordinated to the iron through the nitrogen atom. The complexes were also precipitated in the form of the respective zinc salts; the analysis of these complexes revealed a molar Fe/Zn ratio of 1, thus confirming the charge of the complex anions to be −2. The ionization constants of the aldoxime group in the free ligands and in the respective cyano complexes were also determined. Despite the presence of two donor sites in 1-phenacylpyridinium-4-aldoxime chloride, only the aldoxime group was found to be reactive.

1. Introduction

Compounds that have an amphoteric aldoxime group (>C=N–OH), including the slightly basic nitrogen and the mildly acidic hydroxyl group, are known to form complexes with a great number of metal ions [1–3], as well as with the aquapentacyanoferrate(II) ion, $[Fe(CN)_5OH_2]^{3-}$ [4–12]. Many of these compounds and their metal complexes have shown significant and versatile bioactivities, which are evidently closely related to their chelating ability [13]. They can generally assume the form of two different configuration isomers (*E* and *Z*). The mono- and bis-pyridinium type aldoximes are particularly potent reactivators of the human blood acetylcholinesterase, and thus they are efficient protectors of this enzyme upon phosphorylation by poisons such as pesticides and warfare agents [13]. The cytotoxic and antiproliferative effects of one of the ligands of interest (1-phenacylpyridinium-4-aldoxime chloride) in the SH-SY5Y human neuroblastoma cell line, which is characterized by a high expression of acetylcholinesterase, have been previously observed [14]. The substituted low-spin species of iron, $[Fe(CN)_5L]^{n-}$, in the mononuclear and polynuclear forms, were the subject of numerous investigations mainly as models for active sites in biological macromolecules (porphyrines, cytochromes) and as representatives of supramolecular systems [15–18].

1-Benzylpyridinium-4-aldoxime chloride (BPA4-Cl) and 1-phenacylpyridinium-4-aldoxime chloride (FEPA4-Cl) are representative of the quaternized derivatives of pyridine-4-aldoxime (Scheme 1). Despite their common aldoxime group, considerable differences concerning the reactivity of pyridinium-4-aldoximes and pyridine-4-aldoxime toward $[Fe(CN)_5OH_2]^{3-}$ have been found [7,10–12]. Molecules of the 1-phenacylpyridinium type can be subject to keto-enol tautomerism, but ketones in their solutions appear in equilibrium with an insignificant amount of the enol form [19]. Regarding the reactivity of the carbonyl group, previously performed examinations of the reactions of $[Fe(CN)_5OH_2]^{3-}$ with oxo-oximes, more precisely naphthoquinone oximes, revealed participation of both the carbonyl and the oxime group in complex formation [8]. Recently, certain ketones of the phenacyl- and benzoylethyl-pyridinium type were also found to react with $[Fe(CN)_5OH_2]^{3-}$ [9,20].

To recognize the reactive forms and the stability of the cited ligands in aqueous solutions, the previous scarce characterization [21] was reexamined and extended. Thus, a comparative study concerning the coordination ability of the ligands of interest (BPA4-Cl and FEPA4-Cl) toward the pentacyanoferrate(II) moiety was performed, with special regard to establish which of the two potential donor sites of FEPA4-Cl actually reacts with $[Fe(CN)_5OH_2]^{3-}$. A detailed structural characterization of the two ligands and their complexes with $[Fe(CN)_5OH_2]^{3-}$ in solution and in the solid state was performed using UV–Vis, NMR (^1H and ^{13}C)

* Corresponding author. Tel.: +385 1 4566 760; fax: +385 1 4590 236.
E-mail address: bforetic@mef.hr (B. Foretić).

0020-1693/$ - see front matter © 2010 Elsevier B.V. All rights reserved.
doi:10.1016/j.ica.2010.01.041

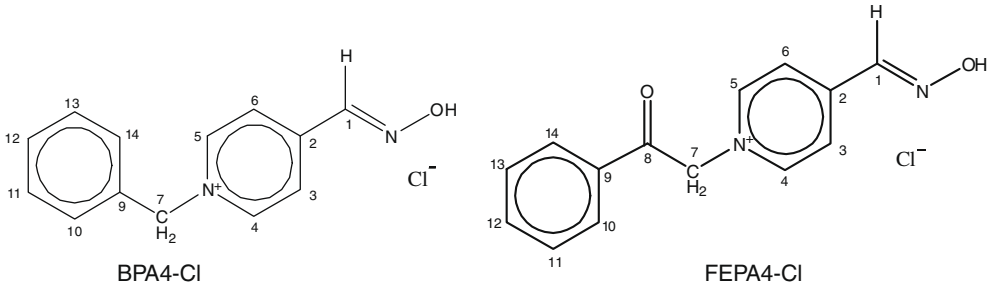

Scheme 1. Assignment of the ligands: 1-benzylpyridinium-4-aldoxime chloride (BPA4-Cl) and 1-phenacylpyridinium-4-aldoxime chloride (FEPA4-Cl).

and FT-IR spectra, as well as X-ray diffraction in the case of the ligands. The isolated complexes were re-precipitated in the form of their respective zinc salts, and the metals were analyzed by particle induced X-ray emission spectroscopy (PIXE).

2. Experimental

2.1. Materials and instruments

Sodium amminepentacyanoferrate(II), $Na_3[Fe(CN)_5NH_3]\cdot 3H_2O$, (Sigma–Aldrich) was recrystallized from a concentrated ammonia solution. Solutions of $[Fe(CN)_5OH_2]^{3-}$ were obtained by aquation of $[Fe(CN)_5NH_3]^{3-}$; the solutions were freshly prepared at room temperature and kept in the dark to minimize dimerization and photolytic and thermal decomposition. The starting materials for the ligand synthesis were reagent grade Aldrich products and were used as purchased. Britton and Robinson buffers were prepared by mixing 100 mL of phosphoric, boric and acetic acid solution (all 0.04 M) with different volumes of 0.2 M sodium hydroxide. The ionic strength was maintained with sodium chloride. Redistilled water was used throughout.

A pH-meter (Mettler Toledo) with an open junction combination polymer electrode was used for pH measurements accurate to ±0.01 pH units. Melting points were determined by a Stuart SMP3 apparatus with a temperature resolution of 0.1°. C, H and N analyses were performed with a LECO elemental analyzer using the ASTM D 5291 method. UV–Vis spectra were recorded on a UNICAM UV 4 spectrophotometer with thermostatted cell holders and 1 cm silica-glass cells. FT-IR and FT-Raman spectra were recorded on a Perkin Elmer Spectrum GX, Series R spectrometer in the range of 4000–400 cm^{-1} using KBr pellets. The ^1H and ^{13}C NMR spectra were recorded with a Bruker AV-600 spectrometer equipped with 5 mm inverse detection and dual probes, respectively, operating at 600.133 MHz for the ^1H nucleus and 150.917 MHz for the ^{13}C nucleus. The spectra were recorded in D_2O and DMSO-d_6 with tetramethylsilane as the internal standard. The HMQC spectra were measured in pulsed field gradient mode (*z*-gradient). The particle induced X-ray emission (PIXE) analysis of the solid zinc salts of the BPA4 and FEPA4 substituted pentacyanoferrate(II) complexes, analyzed as thin targets, were carried out at the Ruđer Bošković Institute. The details of the system have been described previously [22]. The single-crystal X-ray diffraction data were collected on an Oxford Diffraction Xcalibur 3 CCD diffractometer with graphite-monochromated Mo Kα radiation (λ = 0.71073 Å).

2.2. Preparation of BPA4-Cl·H_2O and FEPA4-Cl·H_2O

BPA4-Cl and FEPA4-Cl were prepared according to a general procedure by mixing equimolar ethanol solutions of pyridine-4-aldoxime with benzyl chloride and 2-chloroacetophenone, respectively. The resulting mixtures were left at ambient temperature for approximately seven days. Ether was then added, inducing the formation of white precipitates that were filtered off and purified by recrystallization from ethanol. Transparent, water-soluble single crystals of BPA4-Cl·H_2O (m.p.: 204.9 °C, dec.) spontaneously crystallized from the reaction mixture. Yield, 70.4%. *Anal.* Calc. for $C_{13}H_{13}N_2OCl\cdot H_2O$: C, 58.54; H, 5.67; N, 10.50. Found: C, 58.00; H, 5.53; N, 10.75%. FT-IR (cm^{-1}): ν(O–H)$_{water}$, 3444 (vs); ν(O–H)$_{oxime}$, 3370 (br, vs); ν(C=N)$_{oxime}$, 1644 (vs); ν(C–C, C–N)$_{pyridinium\ ring}$, 1609 (vs), 1522 (vs); ν(NO), 998 (vs). Raman (cm^{-1}): ν(C=N)$_{oxime}$ 1646(s); ν(C–C, C–N)$_{pyridinium\ ring}$, 1612 (vs), 1526 (vs); ν(NO), 1004 (s).

^1H NMR (D_2O, δ): 8.84 (d, J = 6.84 Hz, H-4, H-5), 8.06 (d, J = 6.78 Hz, H-3, H-6), 5.71 (s, H-7), 7.44 (d, J = 7.68 Hz, H-10, H-14), 7.38 (d, J = 7.56 Hz, H-11, H-13), 7.32 (t, J = 7.35 Hz, H-12), 8.23 (s, H-11) ppm. ^1H NMR (DMSO-d_6, δ): 13.02 (s, 1H, OH) ppm.

^{13}C NMR (D_2O, δ): 144.4 (C-4, C-5), 124.9 (C-3, C-6), 148.8 (C-2), 64.2 (C-7), 132.9 (C-9), 129.7 (C-10, C-14), 129.1 (C-11, C-13), 130.0 (C-12), 145.6 (C-1) ppm.

Transparent, water soluble single crystals of FEPA4-Cl·H_2O (m.p.: 206.8 °C) were prepared analogously. Yield, 70.4%. *Anal.* Calc. for $C_{14}H_{13}N_2O_2Cl\cdot H_2O$: C, 57.05; H, 5.13; N, 9.50. Found: C, 57.11; H, 5.15; N, 9.17%. IR (cm^{-1}): ν(O–H)$_{water}$, 3465 (vs); ν(O–H)$_{oxime}$, 3405 (vs); ν(C=O), 1698 (vs); ν(C=N)$_{oxime}$, 1643 (vs); ν(C–C, C–N)$_{pyridinium\ ring}$, 1610 (vs), 1520 (vs); ν(NO), 1001 (vs). Raman (cm^{-1}): ν(C=O), 1704 (m), ν(C=N)$_{oxime}$ 1646(s); ν(C–C, C–N)$_{pyridinium\ ring}$, 1612 (vs), 1526 (s); ν(NO), 1002 (s).

^1H NMR (D_2O, δ): 8.74 (d, J = 6.72 Hz, H-4, H-5), 8.26 (d, J = 6.75 Hz, H-3, H-6), 6.38 (s, H-7), 8.05 (d, J = 7.38 Hz, H-10, H-14), 7.63 (d, J = 7.86 Hz, H-11, H-13), 7.80 (t, J = 7.47 Hz, H-12), 8.40 (s, H-1) ppm. ^1H NMR (DMSO-d_6, δ): 13.10 (s, 1H, OH) ppm.

^{13}C NMR (D_2O, δ): 146.0 (C-4, C-5), 124.5 (C-3, C-6), 149.5 (C-2), 66.6 (C-7), 192.0 (C-8) 132.8 (C-9), 128.4 (C-10, C-14), 129.3 (C-11, C-13), 135.6 (C-12), 146.2 (C-1) ppm.

2.3. Preparation and isolation of BPA4 and FEPA4 substituted pentacyanoferrate(II) complexes

An aqueous solution of 0.124 g of BPA4-Cl (0.5 mmol) in 5–10 mL of water was gradually added to a solution containing 0.033 g of $Na_3[Fe(CN)_5NH_3]\cdot 3H_2O$ (0.1 mmol) in 2 mL of water. The resulting mixture had a pH of about 6. The quickly formed precipitate was filtered off, washed with water and vacuum dried in a desiccator over phosphorus pentoxide. The resulting solid was a dark-blue powder sparingly soluble in water, ethanol and acetone. Qualitative analysis showed that the compound did not contain sodium or chlorine. Yield, 26.1%. *Anal.* Calc. for $(C_{13}H_{13}N_2O)_2[Fe(CN)_5(C_{13}H_{13}N_2O)]\cdot 3H_2O$: C, 60.07; H, 5.16; N, 17.51. Found: C, 59.74; H, 5.25; N, 17.07%.

The IR spectrum undoubtedly showed the occurrence of the free BPA4 cation present as the counter ion. IR (cm^{-1}): ν(OH)$_{water}$ + ν(OH)$_{oxime}$, 3420 (br, vs); ν(C≡N)$_{cyano}$, 2048 (vs); ν(C=N)$_{oxime}$, 1640 (vs); ν(C–C, C–N)$_{pyridinium\ ring}$, 1616 (s), 1518 (m); ν(NO), 1016 (br, vs), 998 (sh, vs).

The NMR spectra were taken quickly after dissolving the complex to prevent possible decomposition. The spectra were dominated by intense signals of the uncoordinated BPA4 cation, causing low or undetectable signals of coordinated BPA4 in the ^{1}H NMR spectrum; meanwhile, the majority of ^{13}C NMR shifts of coordinated and uncoordinated ligands were distinguishable. ^{13}C NMR (D_2O, δ) of the complex anion: 146.2 (C-4, C-5), 126.5 (C-3, C-6), 148.7 (C-2), 129.6 (C-10, C-14), 129.3 (C-11, C-13), 130.1 (C-12), 145.6 (C-1), 166.6 (*cis*-C≡N), 164.0 (*trans*-C≡N) ppm.

The other complex with FEPA4 was prepared in an analogous way by mixing aqueous solutions containing 0.138 g of FEPA4-Cl (0.5 mmol) and 0.033 g of $Na_3[Fe(CN)_5NH_3]\cdot 3H_2O$ (0.1 mmol). Yield, 32.7%. *Anal.* Calc. for $(C_{14}H_{13}N_2O_2)_2[Fe(CN)_5)(C_{14}H_{13}N_2O_2)]\cdot 3H_2O$: C, 58.57; H, 4.71; N, 15.99. Found: C, 58.74; H, 4.54; N, 16.33%.

Likewise, the IR spectrum undoubtedly showed the occurrence of the free FEPA4 cation. IR (cm^{-1}): $\nu(OH)_{water} + \nu(OH)_{oxime}$, 3420 (br, vs); $\nu(C{\equiv}N)_{cyano}$, 2059 (vs); $\nu(C{=}O)$, 1695 (vs), 1699 (vs); $\nu(C{=}N)_{oxime}$, 1645 (vs); $\nu(C{-}C, C{-}N)_{pyridinium\ ring}$, 1616 (s), 1520 (m); $\nu(NO)$, 1019 (s), 999 (s).

The NMR spectra were of poor quality because of insufficient solubility of the complex in water, and thus the spectra were not reliable for interpretation.

2.3.1. Isolation of zinc salts of the substituted pentacyanoferrate(II) complexes

The zinc salts of the substituted pentacyanoferrate(II) complexes were isolated by addition of a few milliliters of an acetic acid solution of zinc nitrate [23] to about 30 mL of a saturated water solution of each of the complex solids. The instantaneously formed gelatinous red-violet precipitates were then filtered off, washed with about 100 mL of water until neutral reaction and dried in vacuo. The mass ratio of Fe and Zn was determined in a homogenous fine powder by PIXE analysis, and for both complexes, the ratio was found to be 0.74 with a statistical error of less than a few percent. This is close to the molar ratio of 1 and concurrent with the formulas $Zn[Fe(CN)_5(C_{13}H_{13}N_2O)]$ and $Zn[Fe(CN)_5(C_{14}H_{13}N_2O_2)]$. $Zn[Fe(CN)_5(C_{13}H_{13}N_2O)]$ IR: $\nu(C{\equiv}N)_{cyano}$, 2086 (vs); $\nu(C{=}N)_{oxime}$, 1635 (m); $\nu(NO)$, 1002 (w). $Zn[Fe(CN)_5(C_{14}H_{13}N_2O_2)]$ IR (cm^{-1}): $\nu(C{\equiv}N)_{cyano}$, 2087 (vs); $\nu(C{=}O)$, 1699 (w), $\nu(C{=}N)_{oxime}$, 1635 (m); $\nu(NO)$, 992 (vw).

2.4. X-ray crystallographic study

The single-crystal X-ray diffraction data of BPA4-Cl·H_2O and FEPA4-Cl·H_2O were reduced and corrected using the CrysAlis software package [24]. Solution, refinement and analysis of the structure was performed using the programs integrated in the WinGX system [25]. Data for BPA4-Cl·H_2O were collected at room and low temperature using two different crystals. Only the low-temperature data are presented here because it was of better quality. Both structures were solved by direct methods. Refinement was performed by the full-matrix least-squares method based on F^2 against all reflections using SHELXL-97 [26]. The non-hydrogen atoms were refined anisotropically. All hydrogen atoms were located in the difference Fourier maps. However, because of poor geometry for some of them, they were placed in calculated positions and refined using the riding model. In both structures, the hydrogen atoms on the hydroxyl groups were placed and refined using the rotating group refinement procedure (the torsion angles that maximized the electron density were chosen), and the hydrogen atoms on the water molecules were placed as found in the map and were refined with restraints. The crystal of BPA4-Cl·H_2O was found to be a racemic twin (same as the crystal with room-temperature data) and was refined using TWIN and BASF instructions. The twin ratio was 0.36(4):0.64(4). An attempt was made to refine the structure in the $P2_1/c$ space group, but it did not converge well and gave an R value of 0.17. The chlorine ion and water molecule would be disordered at the two sites, whereas in $P2_1$, they were clearly resolved. Geometrical calculations were done using PLATON [27]. Drawings of the structures were done using the PLATON and MERCURY [28] programs. The crystallographic data are summarized in Table 1.

Table 1
Crystallographic data for BPA4-Cl·H_2O and FEPA4-Cl·H_2O.

	BPA4-Cl·H_2O	FEPA4-Cl·H_2O
Formula	$C_{13}H_{15}ClN_2O_2$	$C_{14}H_{15}ClN_2O_3$
Formula weight	266.72	294.73
Crystal color, habit	colorless, plate	colorless, prism
Crystal size (mm^3)	0.08 × 0.26 × 0.31	0.30 × 0.31 × 0.40
Crystal system	monoclinic	monoclinic
Space group	$P2_1$	$P2_1/n$
Unit cell parameters		
a (Å)	8.1459(2)	10.2499(3)
b (Å)	11.3603(2)	12.9070(3)
c (Å)	14.0928(3)	11.4331(4)
α (°)	90	90
β (°)	98.976(2)	105.841(3)
γ (°)	90	90
V (Å^3)	1288.18(5)	1455.10(7)
Z	4	4
D_{calc} (g cm^{-3})	1.375	1.345
T (K)	120	100
ρ (Å)	0.71073	0.71073
μ (mm^{-1})	0.292	0.271
F(0 0 0)	560	616
Number of collected data	13 121	14 958
Number of unique data [$F_o \geqslant 4\sigma(F_o)$], R_{int}	6799, 0.020	2553, 0.035
Number of parameters	340	193
R_1[a], wR_2[b] [$F_o \geqslant 4\sigma(F_o)$]	0.0392, 0.0924	0.0372, 0.0530
R_1, wR_2 [all data]	0.0480, 0.0948	0.0920, 0.1004
Goodness of fit (GOF) on F^2, S[c]	0.987	1.003
Minimum and maximum electron density (e Å^{-3})	−0.213, 0.365	−0.221, 0.438

[a] $R = \sum ||F_o - F_c|| / \sum |F_o|$.
[b] $wR = [\sum (F_o^2 - F_c^2)^2 / \sum w(F_o^2)^2]^{1/2}$.
[c] $S = \sum [w(F_o^2 - F_c^2)^2 / N_{obs} - N_{param})]^{1/2}$.

3. Results and discussion

3.1. The crystal structures of FEPA4-Cl·H_2O and BPA4-Cl·H_2O

There were two independent cations of benzylpyridinium-4-aldoxime, two chloride ions and two water molecules in the asymmetric unit of the crystal structure of BPA4-Cl·H_2O (one cation, anion and a H_2O molecule are shown in Fig. 1). The structure of another BPA4 salt, anhydrous 1-benzylpyridinium-4-aldoxime bromide (BPA4-Br), was published recently [29]. The molecular structure of FEPA4-Cl·H_2O is shown in Fig. 2. Its asymmetric unit contains a 1-phenacylpyridinium-4-aldoxime cation, a chloride anion and a water molecule of crystallization. The selected bond distances and angles for both structures are listed in Table 2. The arrangement of the substituents around the C=N bond in the cations of the structures of BPA4-Cl·H_2O, FEPA4-Cl·H_2O, and BPA4-Br shows that the aldoxime is in the *E* configuration. There are only four other structures that contain the pyridinium-4-aldoxime moiety, and all are *E* isomers [30–33].

Analysis of the Cambridge Structural Database (CSD) [34] was performed for the structures that contain the aldoxime unit (structures containing metal atoms were not included). There were 199 structures found (only two protonated on the nitrogen atom), of which only 20 structures were in the *Z* configuration. One outlier (structure EZEGUL) and the protonated structures were suppressed

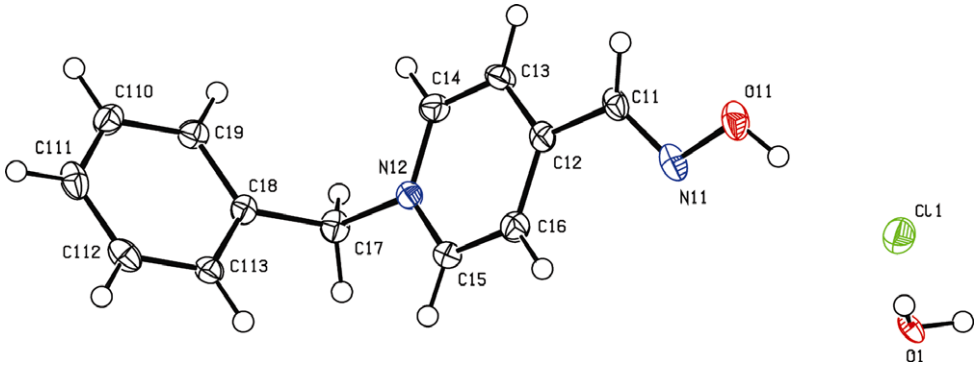

Fig. 1. Drawing of one benzylpyridinium-4-aldoxime cation, one chloride anion and one water molecule of crystallization in the structure of BPA4-Cl·H_2O with the atom numbering scheme. An analogous labeling scheme is used for the other independent cation (O21, N21, N22, C21-C213), anion (Cl2) and water molecule (O2).

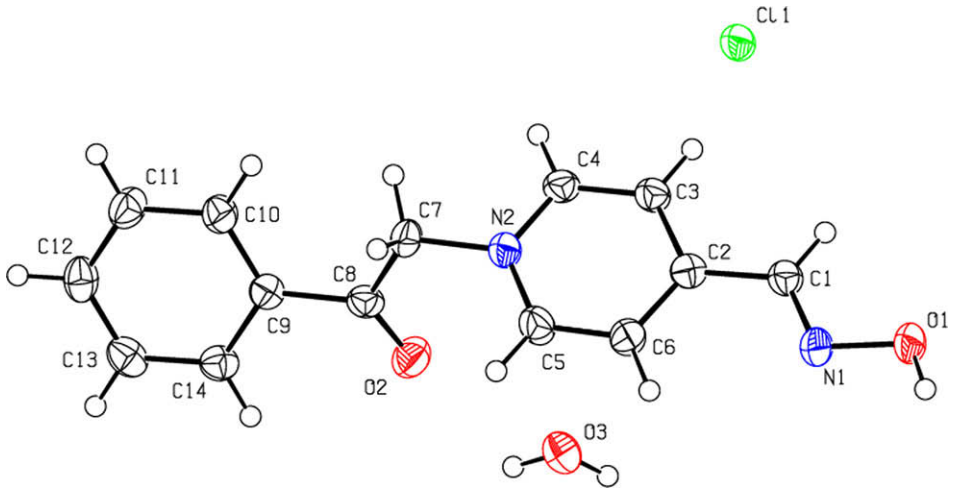

Fig. 2. Drawing of FEPA4-Cl·H_2O with the atom numbering scheme.

Table 2
Selected bond lengths (Å) and angles (°) for FEPA4-Cl·H_2O and two independent molecules in BPA4-Cl·H_2O.

	FEPA4-Cl·H_2O	BPA4-Cl·H_2O cation 1[a]	BPA4-Cl·H_2O cation 2[b]
N1–O1	1.3884(19)	1.386(2)	1.390(2)
C1–N1	1.277(2)	1.293(3)	1.272(3)
C1–C2	1.454(3)	1.470(3)	1.469(3)
C2–C6	1.394(3)	1.398(3)	1.394(3)
C4–N2	1.343(2)	1.345(3)	1.340(3)
C5–N2	1.348(2)	1.348(2)	1.351(3)
C7–N2	1.477(2)	1.502(2)	1.479(3)
C8–O2	1.212(2)		
N1–C1–C2	118.80(18)	118.52(19)	119.28(18)
N2–C7–C8	112.30(15)	111.11(15)	112.03(16)
C1–N1–O1	111.35(16)	110.58(17)	110.55(17)
C4–N2–C5	120.71(16)	121.24(17)	120.52(18)

[a] Numbering of molecule 1 of BPA4-Cl·H_2O begins with digit 1 (N1–O1 in FEPA4-Cl·H_2O is N11–O11 in BPA-Cl·H_2O, molecule 1).
[b] Numbering of molecule 2 of BPA4-Cl·H_2O begins with digit 2 (N1–O1 in FEPA4-Cl·H_2O is N21–O21 in BPA4-Cl·H_2O, molecule 2).

Table 3
Hydrogen bonds (Å, °) in BPA4-Cl·H_2O and FEPA4-Cl·H_2O.

D–H···A	D–H	H···A	D···A	D–H···A
BPA4-Cl·H_2O				
O1–H1A···Cl2^{i}	0.80	2.45	3.2320(15)	166
O1–H1B···Cl1	0.78	2.47	3.2445(14)	172
O2–H2A···Cl2	0.80	2.36	3.1365(14)	167
O2–H2B···Cl1	0.79	2.38	3.1634(2)	175
O11–H11···Cl1^{ii}	0.84	2.14	2.9612(17)	165
O21–H21···O2^{iii}	0.84	1.84	2.693(2)	174
FEPA4-Cl·H_2O				
O1–H1O···Cl1^{iv}	0.88(4)	2.16(4)	3.0389(16)	175(3)
O3–H31···Cl1i^{v}	0.87(3)	2.35(3)	3.2194(18)	176(2)
O3–H32···Cl1^{vi}	0.90(3)	2.28(3)	3.1726(19)	171.2(19)

Symmetry transformation of the asymmetric unit: (i) $1+x, y, z$; (ii) $1-x, y-3/2, 1-z$; (iii) $1-x, 1/2+y, 1-z$; (iv) $x-1/2, 1/2-y, z-1/2$; (v) $1/2+x, 1/2-y, 1/2+z$; (vi) $1/2-x, y-1/2, 3/2-z$.

for analysis. The mean value of the C=N bond in the 242 aldoxime units was 1.271(1) Å (range 1.224–1.309 Å), and the mean value for the N–O bond was 1.396(1) Å (range 1.333–1.434 Å). The C=N–O angle was in the range of 104.6–121.2° with a mean value of 111.7(1)°. As can be seen from the bond lengths and angles for the BPA4 and FEPA4 cations given in Table 4, they are all close to these mean values.

The aromatic rings in the two independent BPA4 cations in the chloride structure are inclined at angles of 70.43(11)° (molecule 1) and 69.69(10)° (molecule 2), while the planes through the phenyl ring (including C8) and the pyridinium-4-aldoxime ring (including C7) in the FEPA4-Cl·H_2O structure form an angle of 50.22(9)°. In the two crystal structures, along with the ionic interactions, a similar hydrogen bonding pattern was formed: there were three hydrogen

Table 4
Ionization constants and molar absorption coefficients of the predominant ionic forms of BPA4 and FEPA4 in aqueous solution ($c = 4 \times 10^{-5}$ M, $I = 0.1$ M, $t = 25$ °C).

Ligand	λ_{max} (nm)	$\varepsilon(H_2L)_{max}$ (M^{-1} cm^{-1})	$\varepsilon(HL)_{max}$ (M^{-1} cm^{-1})	$\varepsilon(L)_{max}$ ($M^{-1}cm^{-1}$)	$pK_{a(aldoxime)}$	$pK_{a(carbonyl)}$
BPA4	283		16 194		8.76 ± 0.02	
	342			24 280		
FEPA4	283	23 330			8.72 ± 0.07	11.40 ± 0.20
	345		27 800	8190		
	440			17 500		

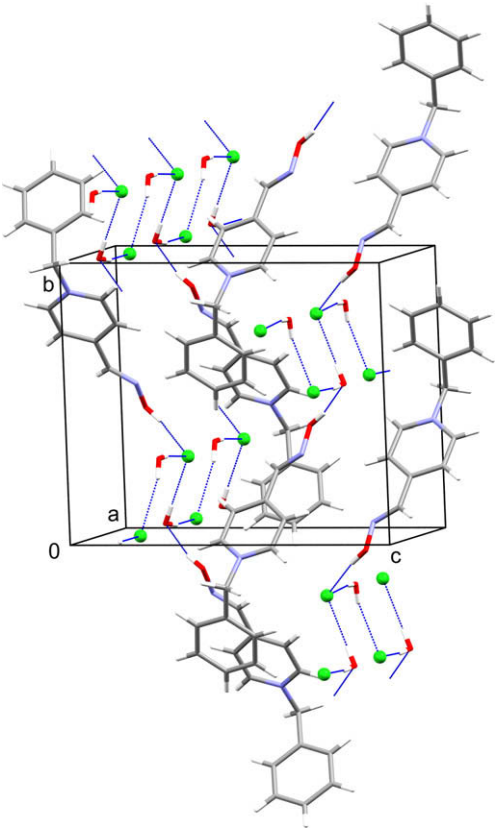

Fig. 3. Packing of BPA4 cations, chloride anions and water molecules in the unit cell of BPA4-Cl·H_2O. Hydrogen bonds are shown by blue dashed lines. (For interpretation of the references to colour in this figure legend, the reader is referred to the web version of this article.)

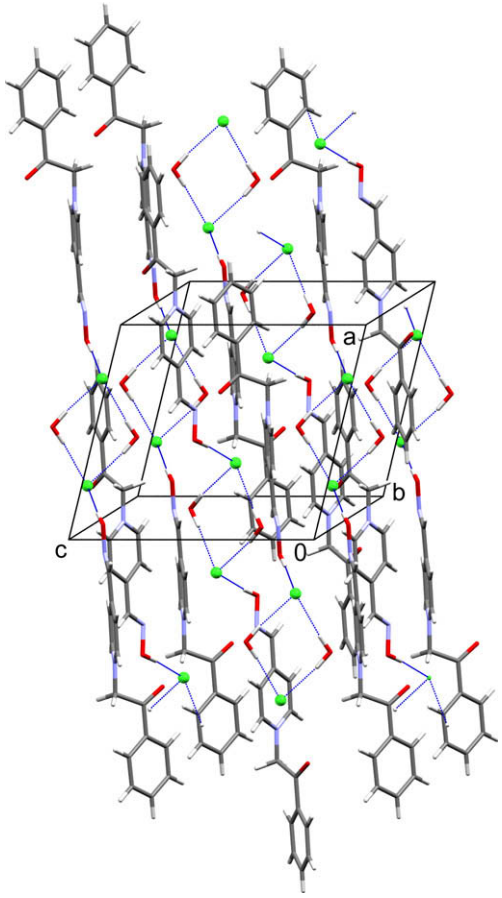

Fig. 4. Packing of FEPA4 cations, chloride anions and water molecules in the unit cell of FEPA4-Cl·H_2O. Hydrogen bonds are shown by blue dashed lines. (For interpretation of the references to colour in this figure legend, the reader is referred to the web version of this article.)

bonds of the O–H···Cl type interconnecting the cations, chloride anions and water molecules (Figs. 3 and 4, Table 3). In both structures, the water molecule was a hydrogen bond donor toward the two chloride anions, where the two chloride anions were independent in BPA4-Cl·H_2O and centrosymmetrically related in FEPA4-Cl·H_2O. In BPA4-Cl·H_2O, the aldoxime hydroxyl group from one molecule formed a hydrogen bond with one chloride ion, while the hydroxyl group from the other molecule was a hydrogen bond donor towards a water molecule. As a result, the anions and water molecules are interconnected into chains through hydrophilic tunnels in the crystal structure (Fig. 3). Quite differently, in the anhydrous structure of BPA4-Br, there was only one O–H···Br hydrogen bond, while the rest were weak interactions including C–H···Br and C–H···π [24]. In FEPA4-Cl·H_2O, the aldoxime hydroxyl group was a hydrogen bond donor only to a chloride ion (Fig. 4). The two aromatic rings, phenyl and pyridine, form π···π interactions with distances between their centroids (Cg1(N2,C2–C6)···Cg2(C9–C14) [$x - 0.5$, $0.5 - y$, $z - 0.5$] of 3.859(1) Å, slippage 1.443(1) Å.

3.2. Electronic absorption spectroscopy

3.2.1. Aqueous solutions of BPA4-Cl·H_2O and FEPA4-Cl·H_2O

The absorption spectra of both ligands exhibited two intensive pH-dependent bands as a result of $\pi \rightarrow \pi^*$ transitions within the pyridiniumaldoxime aromatic system [35]. The maximum at 280 nm was characteristic of the protonated pyridiniumaldoxime group, while the maximum at about 340 nm was due to the absorption of the deprotonated pyridiniumaldoxime group. Both maxima are in accordance with the ^1L_b absorption band of the substituted pyridine ring. The weak band centered on 250 nm was also attributed to the deprotonated pyridiniumaldoxime and is in accordance with the so-called second band (2nd) of the pyridiniumaldoxime aromatic system. These pH-dependent spectral changes exhibited excellent isobesticity. The cation of FEPA4 contains two isolated chromophores: acetophenone and N-methylpy-

ridinium-4-aldoxime. Thus its aqueous solutions exhibited the bands compatible with the linear summation of the respective chromophores: the characteristic intensive conjugation band (or *K* band), according to the intramolecular charge transfer in acetophenone, appearing at 254 nm and the bands associated with absorptions of the pyridiniumaldoxime aromatic system appearing at 283 nm and 345 nm (^1L_b band). In basic aqueous solutions, an additional conjugation band arose at 440 nm as a result of the intramolecular charge transfer between the enolate form of acetophenone and the deprotonated pyridiniumaldoxime part of the molecule. Whereas molecules of the 1-phenacylpyridinium type can be subject to keto-enol tautomerism, it must be pointed out that there was no detectable absorption of the enol chromophore in the examined aqueous solutions of FEPA4, as previously suggested [21]. The predominance of the keto isomer in aqueous solutions of FEPA4 is in accordance with the very small equilibrium ratio of the enol to keto tautomer found for 1-phenacylpyridinium bromide ($pK_T = 6.10$), since it seems that substituents in the pyridine ring have an insignificant effect on the tautomeric equilibria of compounds of the 1-phenacylpyridinium type [19]. Moreover, the low acidity ($pK_a > 10$) of these compounds in comparison with the 2-, 3- and 4-phenacylpyridinium isomers [19] is in accordance with the acidity found for the FEPA4. However, the rapid base-catalyzed first-order decomposition of the enolate ion observed for the 1-phenacylpyridinium cation ($k = 7.1\ s^{-1}$ at pH 12) [19] was considerably slower (~1000 times) for the corresponding ion of FEPA4, $k = (7.4 \pm 0.8) \times 10^{-4}\ s^{-1}$ at pH 12 and 25 °C, because of resonance stabilization through the whole structure. The corresponding schemes of the acid–base equilibria occurring in BPA4 and FEPA4 aqueous solutions are presented in Scheme 2.

The spectral characteristics of the respective ionic forms and the ionization constants of the aldoxime and carbonyl groups derived from absorbance versus acidity curves (Fig. 5) are presented in Table 4. A non-linear regression of the absorbance versus pH data according to Eq. (1) was used. In the case of the overlapping ionization constants for the aldoxime and carbonyl group in FEPA4, Eq. (2) was applied.

$$A = \frac{A\ (\mathrm{HL}) \cdot [\mathrm{H^+}] + A(\mathrm{L}) \cdot K_{\mathrm{a(aldoxime)}}}{[\mathrm{H^+}] + K_{\mathrm{a(aldoxime)}}} \quad (1)$$

$$A = \frac{A(\mathrm{H_2L}) \cdot [\mathrm{H^+}]^2 + A(\mathrm{HL}) \cdot K_{\mathrm{a(aldoxime)}} \cdot [\mathrm{H^+}] + A(\mathrm{L}) \cdot K_{\mathrm{a(aldoxime)}} \cdot K_{\mathrm{a(carbonyl)}}}{[\mathrm{H^+}]^2 + K_{\mathrm{a(aldoxime)}} \cdot [\mathrm{H^+}] + K_{\mathrm{a(aldoxime)}} \cdot K_{\mathrm{a(carbonyl)}}} \quad (2)$$

3.2.2. Aqueous reaction mixtures of BPA4 and FEPA4 substituted pentacyanoferrates(II)

1-Benzylpyridinium-4-aldoxime chloride and 1-phenacylpyridinium-4-aldoxime chloride reacted with $[Fe(CN)_5OH_2]^{3-}$, forming blue colored substituted pentacyanoferrate(II) complexes with a 1:1 molar ratio. The visible spectra of the complexes, produced in solutions of pH from 5 to 10 and a molar ratio of reactants of 1, were characterized by a broad, intensive maximum centered at approximately 560 (BPA-4) and 570 nm (FEPA-4), respectively, compatible with the metal-to-ligand charge transfer (MLCT), $t_{2g} \rightarrow L_\pi^*$. The band shifted bathochromically about 20 nm upon increasing the pH of the medium over 9, due to the equilibrium:

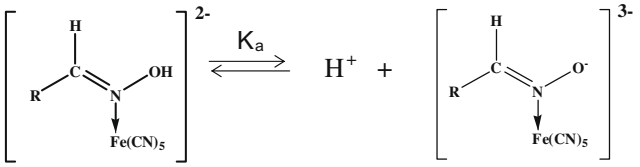

(3)

where R represents the remaining part of the molecules of both ligands. A non-linear least-squares fit of the absorbance versus pH data to Eq. (4) led to the curves presented in Fig. 6 and to the $pK_a = 6.8 \pm 0.1$ for the complex with BPA-4 and $pK_a = 7.2 \pm 0.1$ for the complex with FEPA-4 at 25 °C and $I = 0.1$ M. Calculations were performed at the wavelengths of the corresponding MLCT maxima.

$$A = \frac{A_{\mathrm{protonated}} \cdot [\mathrm{H^+}] + A_{\mathrm{deprotonated}} \cdot K_{\mathrm{a}}}{[\mathrm{H^+}] + K_{\mathrm{a}}} \quad (4)$$

The pK_a values of the coordinated aldoxime groups were reduced by more than one pH unit with respect to the pK_a values of the aldoxime groups in the free ligands, indicating the coordination of both ligands to the iron center through the nitrogen atom [2,3].

The complexes produced in neutral and slightly alkaline solutions exhibited an additional broad maximum or shoulder of lower intensity centered at 450 nm (BPA-4) and 480 nm (FEPA-4). This was also observed in the spectra of other pentacyanoferrate(II) complexes substituted with ligands of the pyridinium aldoxime type [5,10,11]. The band was higher in energy relative to that observed in the 560–580 nm region, and this could suggest the presence of another complex type. Considering the amphoteric character of the aldoxime group, coordination of the aldoxime oxy-

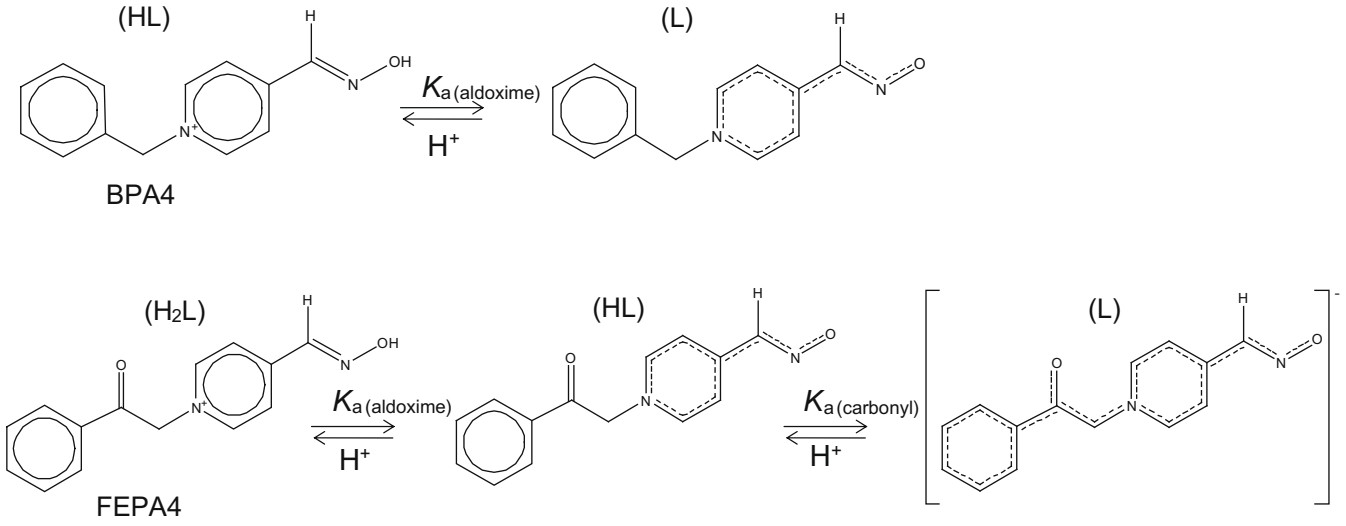

Scheme 2. The acid–base equilibria in BPA4 and FEPA4 solutions.

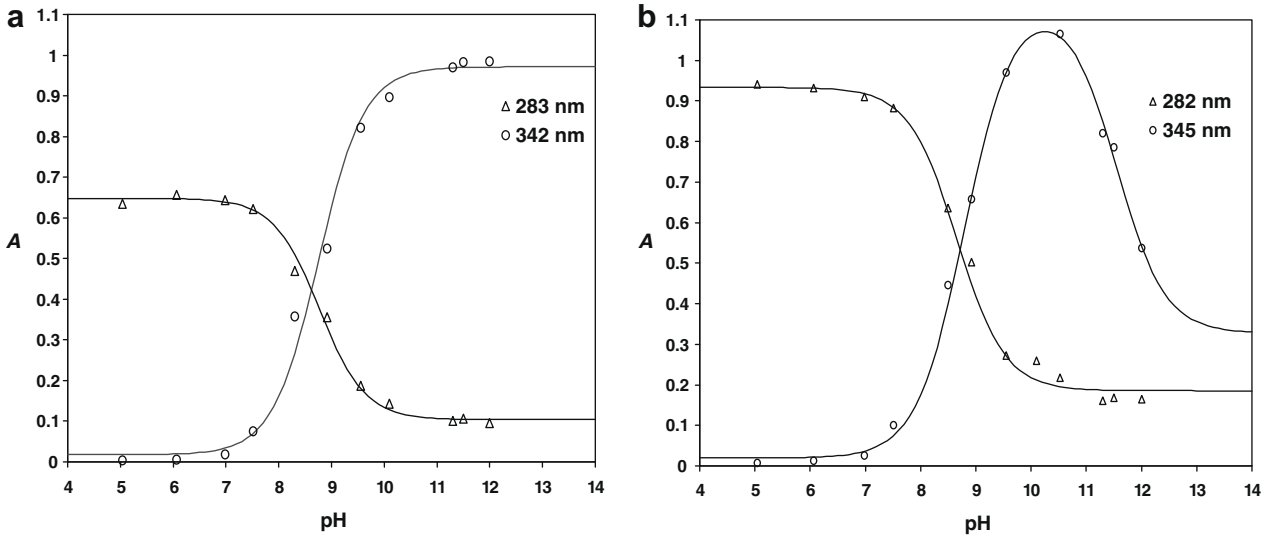

Fig. 5. Absorbance dependence on pH at analytical wavelengths of aqueous solutions of (a) BPA4 and (b) FEPA4 ($c = 4.0 \times 10^{-5}$ M, $t = 25$ °C and $I = 0.10$ M).

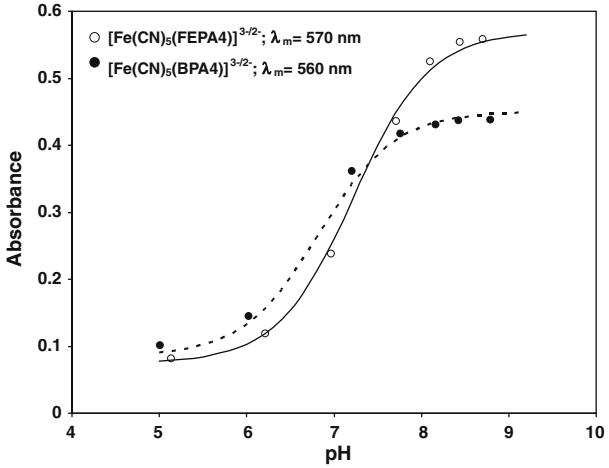

Fig. 6. Absorbance dependence on pH at MLCT wavelengths of aqueous solutions of BPA4 and FEPA4 substituted pentacyanoferrates(II), which were produced by mixing reactants in an equimolar ratio ($c = 5.0 \times 10^{-4}$ M, $t = 25$ °C and $I = 0.10$ M).

gen to the metal center is optional. The band disappeared at higher pH values and in the presence of excess ligand. Therefore, attempts to isolate the complex were unsuccessful.

3.2.3. Aqueous solutions of the isolated BPA4 and FEPA4 substituted pentacyanoferrates(II)

The electronic spectra of the solutions of the isolated solids are presented in Fig. 7. In the visible region, they exhibited the characteristic MLCT maxima at $\lambda = 560$–590 nm (pH ~ 7; $\varepsilon \sim 3010$ $M^{-1}\,cm^{-1}$ and $\varepsilon \sim 1670\ M^{-1}\,cm^{-1}$ for the complex with BPA4 and FEPA4, respectively), while the UV region was dominated by the bands of the uncoordinated ligands. In neutral media (pH ~ 7), they exhibited intraligand absorptions that were covered at other pH values at about 340 nm ($\varepsilon \sim 2150\ M^{-1}\,cm^{-1}$ for the BPA4 complex and $\varepsilon \sim 1430\ M^{-1}\,cm^{-1}$ for the FEPA4 complex) and 380–440 nm ($\varepsilon \sim 720\ M^{-1}\,cm^{-1}$ and $\varepsilon \sim 1500\ M^{-1}\,cm^{-1}$ for the complex with BPA4 and FEPA4, respectively), which was assigned to $\pi \rightarrow \pi^*$ transitions.

3.3. IR spectroscopy

The IR spectra of BPA4-Cl·H_2O and FEPA4-Cl·H_2O exhibited strong absorption bands centered at 3370 cm^{-1} and 3405 cm^{-1}, assigned to the OH stretching of the aldoxime groups. The bands at 3444 cm^{-1} and 3465 cm^{-1}, also appearing in that spectral region, were the result of crystal water OH stretchings. The position and the shape of these bands are in accordance with the hydrogen bond networking of the aldoximic –OH group, Cl^- and H_2O established by X-ray structure analysis. The hydrated BPA4 and FEPA4 substituted pentacyanoferrate(II) complexes displayed a strong and broad band centered at 3420 cm^{-1}, representing an overlapping combination of the O–H stretches of both the water and the aldoxime group.

Bands due to the aldoxime C=N stretchings, occurring at ca. 1625 cm^{-1} for aliphatic aldoximes, were shifted to higher values for aromatic aldoximes, i.e., to about 1644 cm^{-1} in the present cases [36]. These C=N stretches generally shift to lower frequencies upon the coordination of the aldoxime nitrogen to a metal ion [37]. This is not pronounced in the spectra of the current complexes, since the shifts were obscured by the strong absorption of the uncoordinated ligands present in a great portion as cationic counterparts. More illustrative are the spectra of the respective zinc salts, where the C=N stretches appear as medium bands at 1635 cm^{-1}, indicating the aldoxime nitrogen coordination. The relatively small shift in the frequency of the C=N band upon ligation indicated an iron–pyridiniumaldoxime interaction with a predominant σ donation and weak π-back bonding. This is in good correlation with the established low energy of the MLCT transitions.

The ligands displayed very strong absorbances at 998 (BPA4-Cl·H_2O) and 1001 cm^{-1} (FEPA4-Cl·H_2O) that were assigned to the aldoxime N–O stretchings. In the spectra of the BPA4 complex, a strong band occurred at 1016 cm^{-1} with a shoulder at ~998 cm^{-1}, while in the FEPA4 complex, two strong bands at 1019 and 999 cm^{-1} were distinguished. These bands corresponded to the N–O stretchings of the coordinated and uncoordinated ligands, respectively. The shifts of the N–O bands of the coordinated ligands toward higher frequencies are in accordance with the nitrogen coordination to the iron center. In the spectra of the respective zinc salts, the bands in that spectral region were strongly attenuated.

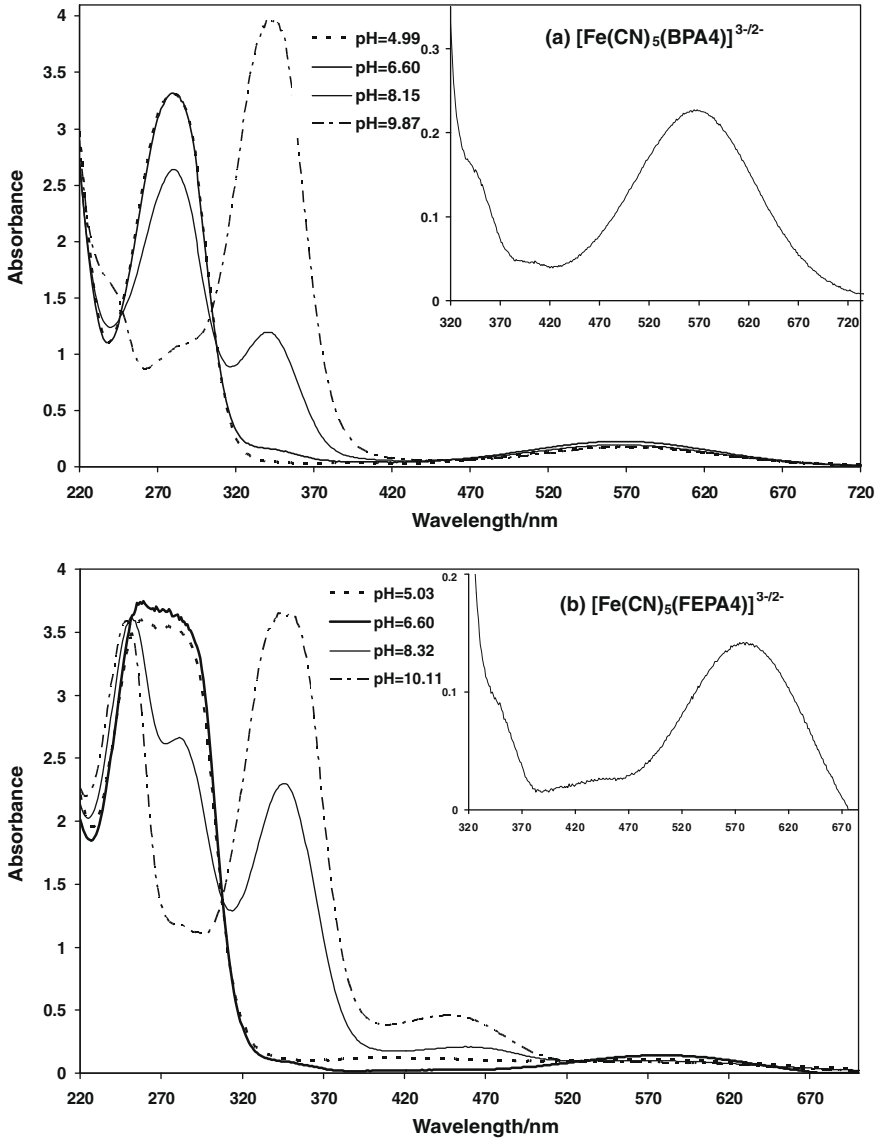

Fig. 7. pH-dependent electronic spectra of the isolated pentacyanoferrates(II), $c = 7 \times 10^{-5}$ M, $I = 0.1$ M, $t = 25$ °C.

In general, the vibrational spectra of the BPA4 and FEPA4 substituted pentacyanoferrates(II) were rather similar, except for the strong band at 1699 cm^{-1} arising from the uncoordinated aromatic ketone C=O stretching, suggesting the analogous mode of coordination of both ligands. The very strong cyanide stretching frequencies, centered at 2048 cm^{-1} and 2059 cm^{-1} for BPA4 and FEPA4 complexes, respectively, were in the range expected for octahedral pentacyanoferrate(II) complexes [16,36].

3.4. Proton and carbon NMR spectroscopy

Nuclear magnetic resonance has been previously used to characterize substituted pentacyanoferrate(II) complexes and to investigate the σ and π bonding Fe–ligand interactions [16]. The assignments of NMR shifts for the free ligands were made by analyzing their 2D HMQC spectra and are found to be in good agreement with literature values established for structurally similar compounds [13,38,39]. The aldoxime protons were not observed in D_2O because of their partial ionization and subsequent exchange with the solvent, but their shifts were observed in DMSO. The presence of exclusively one configuration isomer of both ligands and only the keto tautomer (the C=O signal at 192.0 ppm) of FEPA4 were identified. The NMR shifts of the ligands are discussed in comparison with those of pyridine-4-aldoxime (Scheme 3). The ^{13}C NMR resonance signals indicate the particularities of the electronic structure of the pyridinium cation, with reduced electron density on the nitrogen atom, in relation to pyridine-4-aldoxime. The inductive and mesomeric effects in the electronic density distribution resulted in the large upfield shifts of the two magnetically equivalent carbon atoms adjacent to nitrogen and downfield shifts of the remaining three carbons in the pyridinium ring of BPA4 and FEPA4. The largest deshielding (+9.2 ppm for FEPA4 and +8.6 ppm for BEPA4) occurred at the aromatic carbon atom bound to the aldoxime group due to the contribution of the positive charge formed as a consequence of π-electron resonance stabilization. In the ^1H NMR spectra, this effect is not pronounced with respect to the aromatic hydrogen shifts, but it is clearly manifested in the deshielding effect and downfield shift of the remote hydrogen nucleus in the aldoxime group (13.0 ppm for BPA4, 13.1 ppm for FEPA4 and 11.8 ppm for pyridine-4-aldoxime) included in the resonance stabilization. Such electron distribution in pyridiniumaldoximes clearly explains their higher acidity in

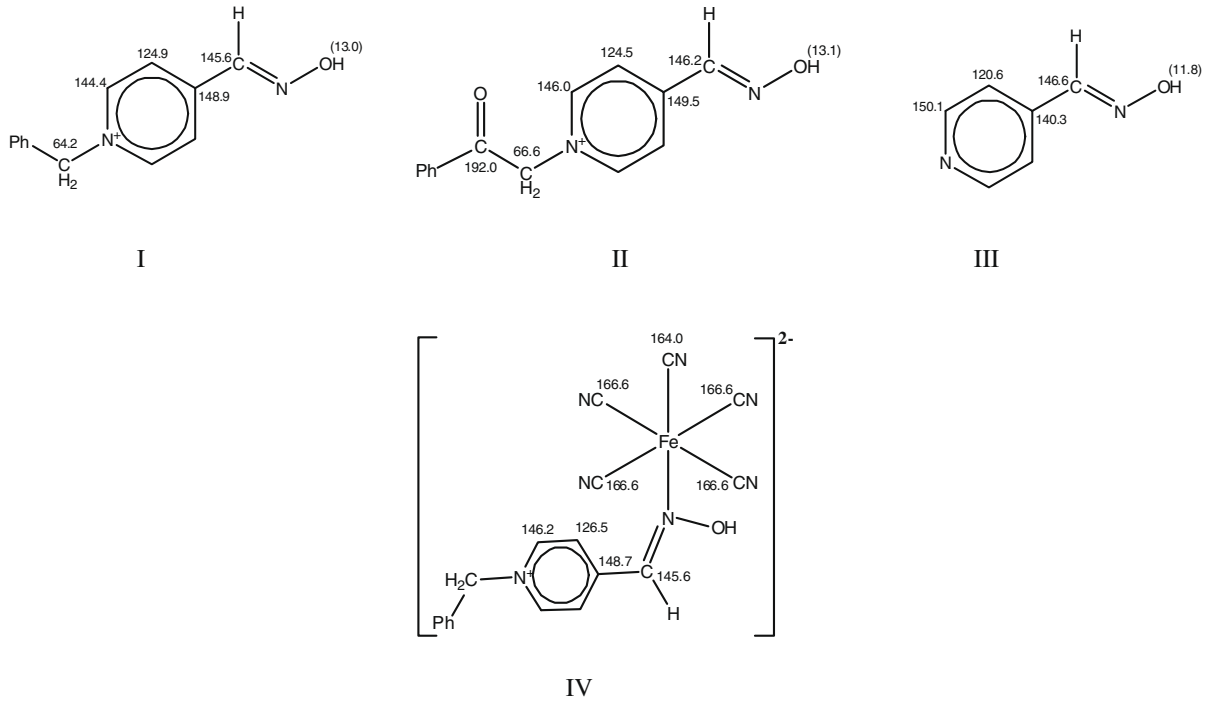

Scheme 3. Selected NMR shifts (^{1}H shifts are given in parentheses) of the I – FEPA4, II – BPA4, III – pyridine-4-aldoxime and IV – BPA4 substituted pentacyanoferrate(II) anion.

aqueous solution (pK_a(FEPA4) = 8.72; pK_a (BPA4) = 8.76) in comparison with pyridine-4-aldoxime (pK_a = 9.99 [40]). This is related to the considerably higher reactivity of the aldoxime group in pyridinium-4-aldoxime compounds toward the aquapentacyanoferrate(II) ions with respect to pyridine-4-aldoxime [6,7,10].

The FEPA4 substituted pentacyanoferrate(II) complex was not sufficiently soluble in D_2O, preventing a reliable spectral interpretation. The ^{1}H and ^{13}C NMR spectra of the BPA4 substituted pentacyanoferrate(II) clearly indicated the presence of the coordinated and uncoordinated ligand. The ^{1}H NMR spectrum was dominated by intensive signals of the uncoordinated BPA4 cation, causing low or undetectable signals of the coordinated cation. The ^{13}C NMR chemical shifts of the pentacyanoferrate(II) anion were assigned in comparison to the shifts of the free ligand. The selected ^{13}C NMR shifts of the BPA4 substituted pentacyanoferrate(II) complex are shown in Scheme 3. The ^{13}C NMR chemical shifts of the coordinated BPA4 in the pentacyanoferrate(II) anion are the result of two major effects: the deshielding effect due to the involvement of σ electrons of aldoxime group in coordination to iron center and the shielding effect due to π-back donation of iron to the aldoxime group. The pronounced σ induction of electron density towards iron(II) ion was manifested as the upfield shifts of the pyridinium carbon atoms. Two cyanide resonance signals, with a ratio of relative intensities of approximately 4:1, were assigned to four *cis*-(166.6 ppm) and one *trans*-configured cyano groups (164.0 ppm), indicating the *trans*-configuration of BPA4 in the octahedral complex. Since the cyano resonance in the hexacyanoferrate(II) ion occurs at 177.0 ppm [16], the upfield shifts of both cyano signals were evident. Such a shielding effect of the carbon nuclei in cyanide groups is a consequence of increased π-back bonding from iron to the cyano ligands and the very poor π-back donation towards the aldoxime group in coordinated BPA4. This observation is in accordance with the low energy wavelength position of the MLCT bands found not only for aqueous solutions of the examined pentacyanoferrate(II) complexes but also for other pyridiniumaldoxime substituted pentacyanoferrates(II), ranging from 500 to 620 nm [5,12].

4. Conclusions

The crystalline monohydrates of 1-benzylpyridinium-4-aldoxime and 1-phenacylpyridinium-4-aldoxime chlorides were prepared and structurally characterized. The arrangement of the substituents around the C=N bond in the cations showed that the aldoxime group is in the *E* configuration. The two presented ligands react with aquapentacyanoferrate(II) ion by forming mononuclear complexes through the coordination of the aldoxime nitrogen to the iron center. The new pentacyanoferrate(II) complexes substituted with the biologically active ligands of interest (BPA4-Cl and FEPA4-Cl) were synthesized and characterized on the basis of elemental analysis and spectroscopic methods. The pentacyanoferrate(II) moiety induced an increase in the acidity of the pyridinium-4-aldoxime ligands, as reflected in the pK_a value of the coordinated aldoxime, which was more than 1 unit lower than the pK_a value of the free aldoxime. This conforms with an electrostatic effect of coordination, i.e., of σ donation and weak π-back bonding. The weak π-back bonding capability of the pyridinium-4-aldoxime ligands resulted in the low energy of the MLCT bands, the IR shifts in C=N and N–O stretching frequencies in comparison with free aldoximes, and the shielding effect of the carbon nuclei in cyano groups in ^{13}C NMR.

Spectral and elemental analyses of the synthesized complexes were in optimal accordance with the formulas {$(BPA4)_2$[$Fe(CN)_5$(BPA4)]}·$3H_2O$ and {$(FEPA4)_2$[$Fe(CN)_5$(FEPA4)]}·$3H_2O$. Analysis of the isolated zinc salts showed a Fe/Zn molar ratio of 1, confirming the charges of the complex anions in the isolated complexes to be −2. Within the two donor groups, aldoxime and carbonyl, present in 1-phenacylpyridinium-4-aldoxime chloride, the aldoxime group is obviously a more favorable and better entering species.

Acknowledgments

Financial support for this research was provided by the Ministry of Science and Technology of the Republic of Croatia (Grant Nos. 108-1193079-3070 and 119-1193079-1084).

Appendix A. Supplementary material

CCDC 735355 and 735356 contain the supplementary crystallographic data. These data can be obtained free of charge via www.ccdc.cam.ac.uk, or from the Cambridge Crystallographic Data Centre, 12 Union Road, Cambridge, CB2 1EZ, UK; fax: (+44) 1223 336 033; or e-mail: deposit@ccdc.cam.ac.uk. Supplementary data associated with this article can be found, in the online version, at doi:10.1016/j.ica.2010.01.041.

References

[1] A. Chakravorthy, Coord. Chem. Rev. 13 (1974) 1.
[2] V.Yu. Kukushkin, A.J.L. Pomberio, Coord. Chem. Rev. 181 (1999) 147.
[3] C.J. Milios, T.C. Stamatatos, S. Perlepes, Polyhedron 25 (2006) 134.
[4] N. Burger, V. Hankonyi, Z. Smerić, Inorg. Chim. Acta 165 (1989) 83.
[5] V. Hankonyi, V. Ondrušek, V. Karas-Gašparec, Z. Binenfeld, Z. Phys. Chem. 251 (1972) 280.
[6] N. Burger, V. Hankonyi, Z. Smerić, Z. Phys. Chem. 271 (1990) 787.
[7] N. Burger, V. Hankonyi, Monatsh. Chem. 124 (1993) 467.
[8] B. Foretić, N. Burger, V. Hankonyi, Polyhedron 14 (1995) 605.
[9] B. Foretić, J. Lovrić, N. Burger, J. Coord. Chem. 59 (2006) 1537.
[10] N. Burger, V. Karas-Gašparec, Talanta 28 (1981) 323.
[11] N. Burger, V. Karas-Gašparec, Talanta 31 (1984) 169.
[12] N. Burger, V. Hankonyi, Anal. Lett. 25 (1992) 1355.
[13] E. Abele, R. Abele, E. Lukevics, Chem. Heterocycl. Compd. 39 (2003) 847.
[14] S.K. Bognar, B. Foretić, Ž. Vukelić, T. Gulin, D. Ježek, Croat. Chem. Acta 81 (2008) 67.
[15] E. Ilkowska, K. Lewiński, R. Van Eldik, G. Stochel, J. Biol. Inorg. Chem. 4 (1999) 302.
[16] D.H. Macartney, Rev. Inorg. Chem. 9 (1988) 101.
[17] H.E. Toma, A.A. Batsta, H.B. Gray, J. Am. Chem. Soc. 104 (1982) 7509.
[18] H. Winnischofer, F.M. Engelmann, H.E. Toma, K. Araki, H.R. Rechenberg, Inorg. Chim. Acta 338 (2002) 27.
[19] A.R.E. Carey, R.A. More O'Ferrall, B.A. Murray, J. Chem. Soc., Perkin Trans. 2 (1993) 2297.
[20] J. Lovrić, B. Foretić, N. Burger, Z. Phys. Chem. 218 (2004) 1289.
[21] V. Hankonyi, Z. Binenfeld, V. Karas-Gašparec, Croat. Chem. Acta 44 (1972) 329.
[22] I. Pucić, T. Madžar, M. Jakšić, Monatsh. Chem. 137 (2006) 953.
[23] E.F.G. Herington, J. Chem. Soc. (1956) 2747.
[24] Oxford Diffraction, Oxford Difraction Ltd., Xcalibur CCD system, CRYSALIS Software system, Version 1.170, 2003..
[25] L.J. Farrugia, J. Appl. Crystallogr. 32 (1999) 837.
[26] G.M. Sheldrick, SHELXL-97, Program for the Refinement of Crystal Structures, University of Göttingen, Germany, 1997.
[27] A.L. Spek, Acta Crystallogr., Sect. A 46 (1990) C34.
[28] L.J. Farrugia, J. Appl. Crystallogr. 30 (1997) 565.
[29] R. Odzak, I. Halasz, S. Tomić, D. Matković-Čalogović, Acta Crystallogr., Sect. E 62 (2006) 2423.
[30] W. van Havere, A.T.H. Lenstra, H.J. Geise, G.R. van den Berg, H.P. Benschop, Acta Crystallogr., Sect. B 38 (1982) 1635.
[31] I. Vicković, L. Pavlić, D. Mrvoš-Sermek, M. Mesić, Z. Kristallogr. 210 (1995) 282.
[32] I. Vicković, M. Mesić, Z. Kristallogr. 211 (1996) 413.
[33] C.D. Bustamante, R.J. Staples, Z. Kristallogr. - New Cryst. Struct. 214 (1999) 141.
[34] F.H. Allen, Acta Crystallogr., Sect. B 58 (2002) 380.
[35] E.S. Stern, C.J. Timmons, Gillam and Stern's Introduction to Electronic Absorption Spectroscopy in Organic Chemistry, Edward Arnold, London, 1970.
[36] K. Nakamoto, Infrared and Raman Spectra of Inorganic And Coordination Compounds, Wiley, New York, 1986.
[37] R. Middleton, J.R. Thornback, G. Wilkinson, J. Chem. Soc., Dalton Trans. (1980) 174.
[38] A. Szwajca, B. Łeska, G. Schroeder, M. Szafran, J. Mol. Struct. 708 (2004) 87.
[39] U. Spöhrer, P. Eyer, J. Chromatogr. A (1995) 55.
[40] S.F. Mason, J. Chem. Soc. (1960) 22.